INTERNATIONAL JOURNAL FOR NUMERICAL METHODS IN ENGINEERING
Int. J. Numer. Meth. Engng 2000; **00**:1–6 *Prepared using* nmeauth.cls *[Version: 2002/09/18 v2.02]*

A space–time discontinuous Galerkin method for the solution of the wave equation in the time-domain

Steffen Petersen, Charbel Farhat*† and Radek Tezaur

Department of Mechanical Engineering and Institute for Computational and Mathematical Engineering, Stanford University, Mail Code 3035, Stanford, CA 94305, USA

SUMMARY

In recent years, the focus of research in the field of computational acoustics has shifted to the medium frequency regime and multiscale wave propagation. This has led to the development of new concepts including the discontinuous enrichment method. Its basic principle is the incorporation of features of the governing partial differential equation in the approximation. In this contribution, this concept is adapted for the simulation of transient problems governed by the wave equation. We present a space–time discontinuous Galerkin method with Lagrange multipliers, where the shape approximation in space and time is based on solutions of the homogeneous wave equation. The use of hierarchical wave-like basis functions is enabled by means of a variational formulation that allows for discontinuities in both the spatial and the temporal discretizations. Numerical examples in one space dimension demonstrate the outstanding performance of the proposed method compared to conventional space–time finite element methods. Copyright © 2000 John Wiley & Sons, Ltd.

KEY WORDS: wave equation; discontinuous Galerkin; Lagrange multipliers; medium frequency; wave basis functions; space–time finite elements

1. INTRODUCTION

A major focus of current research in the field of computational acoustics pertains to the medium frequency regime and multiscale wave propagation. In these cases, the finite element simulation of transient wave propagation phenomena, governed by the wave equation, requires a high resolution of the discretization in space and time. Using standard finite element approaches, this may rapidly exceed the available computer resources, rendering the numerical simulations unfeasible. Hence, high order methods have to be employed in order to efficiently solve wave

*Correspondence to: Department of Mechanical Engineering and Institute for Computational and Mathematical Engineering, Stanford University, Mail Code 3035, Stanford, CA 94305, USA
†E-mail: cfarhat@stanford.edu

Contract/grant sponsor: German Academic Exchange Service (DAAD); contract/grant number: D/06/44695

Contract/grant sponsor: Office of Naval Research (ONR); contract/grant number: N00014-05-1-0204-1

Received XX XXXX 2007
Revised XX XXXX 2007

propagation problems in the time domain. The most promising of such methods may be either found in the field of spectral element methods (see e.g. [1]) or among different variants of the discontinuous Galerkin method (DGM) (see e.g. [2] for a recent approach including higher order approximations in space and time). Based on the latter approach, we present a high order method for the simulation of wave propagation in the time domain.

Regarding the investigation of wave propagation phenomena the DGM has gained considerable popularity in recent years and has meanwhile become an effective approach for solving a wide range of hyperbolic as well as elliptic problems [3, 4, 5]. A comprehensive survey of developments in discontinuous Galerkin methods in the past decades is given in [6]. The most relevant advantages of discontinuous Galerkin formulations include a mechanism for the design of stable and high-order accurate methods (see e.g. [7, 8]), the possibility for using a broad range of approximation functions including solutions of the governing differential equation [9], the formulation of efficient explicit solution schemes [10], and a convenient framework for the application of adaptive mesh refinement techniques [11].

Up to now, various flavors of the discontinuous Galerkin method for the second order wave equation have been developed, where discontinuities may be considered in the spatial discretization [10, 12], in the temporal discretization (which is also sometimes referred to as time discontinuous Galerkin method) [13] or in both [14]. The formulations that consider spatial discontinuities mostly follow the concept of semi-discrete approaches. Hence, a discontinuous Galerkin scheme is used to discretize the problem in space and appropriate time stepping schemes are then used to solve the resulting system of ordinary differential equations [10, 12]. A major advantage of these methods is the fact that the discontinuous approximation leads to block diagonal form of the mass matrix, rendering explicit time integration attractive. In [15] an extensive analysis of the dispersion and dissipation of commonly used discontinuous Galerkin schemes including higher order approximations is given. Quite recently, a method that uses a mixture of standard finite element and discontinuous Galerkin approximations has been proposed in [16].

An effective framework for high-order accurate methods is given by space–time finite element approaches that use standard finite element shape functions to discretize the problem in space and time, while allowing for discontinuities in the temporal discretization [13, 17, 18, 19, 20, 21]. Regarding the wave equation, there are two basic solution concepts. One approach is to deal directly with the second order problem in the sense of a single field formulation [13, 17, 18]. Another approach is to transform the original problem into a system of first order equations, rendering a two field formulation [13, 18, 19, 20, 21]. Clearly, the latter one comes with the disadvantage that the number of unknowns in the resulting system is significantly increased. In order to prove convergence, the space–time element formulation in [13] was derived in the framework of a Galerkin least-squares method. The additional least-squares terms physically include additional dissipation and increase the stability of the time discontinuous Galerkin formulation [13]. Results of a dispersion and dissipation analysis are given in [18]. The formulation has also been adopted and extended for the investigation of acoustic problems [22, 23, 24]. Space–time finite elements in the context of variational multiscale formulations have been presented in [25].

A space–time discontinuous Galerkin method (i.e. allowing for discontinuities in space and time) suitable for solving the wave equation was developed in [26, 27] and has recently been extended in [14]. While standard space–time finite elements generally require an implicit time integration, the space–time DGM presented in [14] leads to a system that can be solved in an

explicit way for certain configurations of the space–time discretization.

With respect to problems of time harmonic wave propagation, the need for computations in the mid-frequency regime has led to the development of higher order methods such as the partition of unity method [28], the ultraweak variational method [29], the flexible local approximation method [30], and the discontinuous enrichment method (DEM) [9]. The basic principle of these methods is to include features of the governing differential equation in the approximation. In the formulation of the DEM, this is accomplished by enriching the polynomial finite element space with solutions of the homogeneous differential equation. For many problems in the frequency domain, the polynomial field may contribute only little to the approximation solution, which motivates a removal of the polynomial field. This transforms the DEM into a discontinuous Galerkin method (DGM) in which the solution is approximated by plane waves and continuity is weakly enforced by means of a Lagrange multiplier field [31]. The DEM and the DGM with Lagrange multipliers have recently proven their efficiency for the simulation of various two-scale wave propagation phenomena in the mid-frequency regime [32, 33, 34] (see also [35] for a derivation of the DEM for multiscale analysis). In the current work, this concept is extended to analyze wave propagation phenomena in the time domain. The use of free space solutions of the wave equation in the shape approximation is enabled by means of a space–time variational formulation that allows for discontinuities in the spatial and temporal discretization. Here, we focus on the flexibility and improvement of the approximation while solving the transient problem implicitly. However, the method may be extended to explicit time integration following the concept of appropriately discretizing the computational domain as explained in [14].

First, the boundary/initial value problem under consideration is briefly stated. The weak formulation presented in section 2.2 is based on the time discontinuous Galerkin method for second order hyperbolic problems given in [17]. However, the formulation is modified in the sense that we also allow for discontinuities in the spatial discretization. This enables the use of basis functions that are solutions of the homogeneous wave equation. The approximation of the field variable and the Lagrange multipliers is addressed in section 3. The proposed simulation procedure includes a static condensation as well as a simplified evaluation of integral terms, which is described in a subsequent section. The outstanding performance of the space–time DGM developed here is then demonstrated for various one-dimensional example problems. Final remarks are given in the conclusions.

2. A SPACE–TIME DISCONTINUOUS GALERKIN METHOD WITH TRANSPORT POLYNOMIALS

A fundamental idea of the DEM is the use of free space solutions in the element approximations. For the acoustic wave equation in one space dimension (1), a free space solution is represented by any function of the form $f(x \pm ct)$, which also represent solutions of the well-known transport equation. An evident choice for the element basis functions are polynomials in terms of $x \pm ct$, representing approximations in both space and time. A similar concept in a continuous setting has been used in the Trefftz type flexible local approximation method (FLAME) [30]. Here, such polynomials are used in a discontinuous setting, which requires an appropriate variational framework that can be found in the formulation of space–time finite elements.

For simplicity, the proposed method is discussed in one space dimension. However, its

expansion to multiple space dimensions is straightforward and follows the work proposed in [31, 33].

2.1. Problem statement

Consider the wave equation in a one dimensional domain Ω, a time interval $I =]0, T[$, and homogeneous Dirichlet boundary conditions on $\partial\Omega \times I$. Initial conditions at $t = 0$ for the field variable $u(x, t)$ and its time derivative are prescribed. Hence, the problem statement reads

$$-u_{xx} + \frac{1}{c^2}\ddot{u} = 0 \quad \text{in} \quad \Omega \times I, \tag{1}$$

$$u = 0 \quad \text{on} \quad \partial\Omega \times I, \tag{2}$$

$$u = U_0 \quad \text{and} \quad \dot{u} = \dot{U}_0 \quad \text{at} \quad t = 0, \tag{3}$$

where we have used the subscript $_x$ and the symbol $\dot{}$ to indicate the derivatives with respect to x and t , respectively.

Using a sequence of discrete time levels $0 = t_0 < t_1 < ... < t_N = T$, the space–time domain is partitioned in N slabs $\Omega \times I_n$, with $I_n =]t_n, t_{n+1}[$. Each slab is then discretized with elements that include approximations in space and time. For simplicity, only structured discretizations in space and time are considered here. The geometry of the problem is depicted in Figure 1.

The trial functions and the weighting functions are allowed to be discontinuous across the slabs. This leads to temporal jump terms

$$[\![u(t_n)]\!] = u(x, t_n^+) - u(x, t_n^-), \tag{4}$$

where

$$u(t_n^\pm) = \lim_{\epsilon \to 0^+} u(t_n \pm \epsilon). \tag{5}$$

Similarly, jump terms corresponding to discontinuities in the spatial direction may be defined by

$$[\![u(\Gamma_{e,e'})]\!] = u(x^+(\Gamma_{e,e'}), t) - u(x^-(\Gamma_{e,e'}), t), \tag{6}$$

where $\Gamma_{e,e'}$ denotes the edge of two neighboring elements e and e' that is fixed in space. This situation is depicted in Figure 2.

2.2. Variational formulation

Our treatment of the temporal discontinuities follows the single-field formulation of the time discontinuous Galerkin method introduced in [13]. The governing differential equation is multiplied by time derivatives of the weighting functions w and integrated over each space–time slab. Essentially, the continuity of u and $\dot{u}$ is weakly enforced by means of energy inner products (cf. [13] and [22] for details). Hence, the variational form of the the problem given in equations (1)–(3) may be written as

$$\int_{t_n}^{t_{n+1}} \int_\Omega (-u_{xx} + \frac{1}{c^2}\ddot{u})\ \dot{w}\ dx\, dt + \int_\Omega \frac{1}{c^2}[\![\dot{u}(t_n)]\!]\ \dot{w}(t_n^+)\ dx + \int_\Omega [\![u_x(t_n)]\!]\ w_x(t_n^+)\ dx = 0. \tag{7}$$

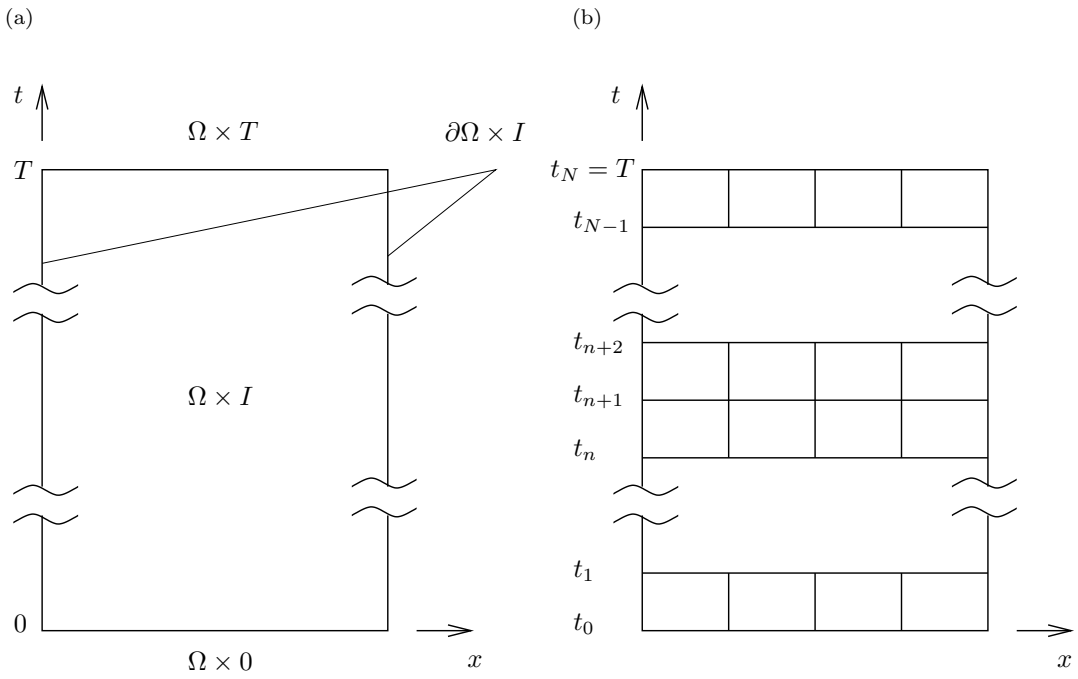

Figure 1. Illustration of space–time finite elements in one space dimension.

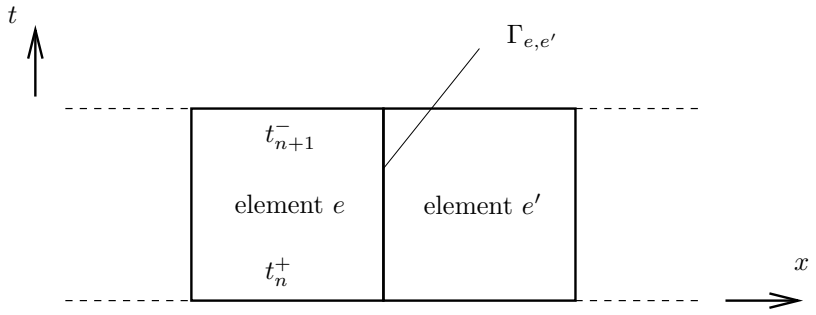

Figure 2. Two neighboring elements within one space–time slab.

Considering a single element that does not share a boundary with $\partial\Omega$. Integration by parts

of the first term in the integral over $\Omega \times I_n$ yields

$$-\int_{t_n}^{t_{n+1}} \int_\Omega u_{xx}\dot{w}\, dx\, dt = -\int_{t_n}^{t_{n+1}} [u_x\ \dot{w}]_{\Gamma_e} dt + \int_{t_n}^{t_{n+1}} \int_\Omega u_x \dot{w}_x\, dx\, dt. \tag{8}$$

Next, the test and trial functions are allowed to be discontinuous in space. Continuity of u is then weakly enforced by means of Lagrange multipliers λ and μ on $\Gamma_{e,e'}$, which leads to the hybrid variational formulation

$$\begin{aligned}
&\int_{t_n}^{t_{n+1}} \int_\Omega (u_x\ \dot{w}_x + \frac{1}{c^2}\ddot{u}\ \dot{w})\, dx\, dt \\
&+ \int_\Omega \frac{1}{c^2} [\![\dot{u}(t_n)]\!]\ \dot{w}(t_n^+)\, dx + \int_\Omega [\![u_x(t_n)]\!]\ w_x(t_n^+)\, dx \\
&+ \sum_e \sum_{e<e'} \int_{t_n}^{t_{n+1}} [\![\dot{w}(\Gamma_{e,e'})]\!]\ \lambda\, dt = 0,
\end{aligned} \tag{9}$$

$$\sum_e \sum_{e<e'} \int_{t_n}^{t_{n+1}} [\![\dot{u}(\Gamma_{e,e'})]\!]\ \mu\, dt = 0. \tag{10}$$

Note that the values of $\dot{u}(t_n^-)$ and $u_x(t_n^-)$ that appear in the jump terms of equation (9) are known from the previous time step, and the corresponding terms may be shifted to the right hand side. Then

$$\begin{aligned}
&\int_{t_n}^{t_{n+1}} \int_\Omega (u_x\ \dot{w}_x + \frac{1}{c^2}\ddot{u}\ \dot{w})\, dx\, dt \\
&+ \int_\Omega \frac{1}{c^2}\dot{u}(t_n^+)\ \dot{w}(t_n^+)\, dx + \int_\Omega u_x(t_n^+)\ w_x(t_n^+)\, dx + \sum_e \sum_{e<e'} \int_{t_n}^{t_{n+1}} [\![\dot{w}(\Gamma_{e,e'})]\!]\ \lambda\, dt \\
&= \int_\Omega \frac{1}{c^2}\dot{u}(t_n^-)\ \dot{w}(t_n^+)\, dx + \int_\Omega u_x(t_n^-)\ w_x(t_n^+)\, dx.
\end{aligned} \tag{11}$$

In the first time step, $\dot{u}(t_n^-)$ is replaced by $\dot{U}_0$, and $u_x(t_n^-)$ can be computed from the initial condition U_0.

3. DISCRETIZATION

In order to obtain a discrete version of the variational form (11) the test and trial functions u and w are replaced by appropriate approximations u^h and w^h. Similarly, the approximations λ^h and μ^h replace λ and μ.

3.1. Transport polynomial approximation of the solution

Following the main concept described in [9], we choose basis functions that are solutions of the homogeneous wave equation. Note that in one space dimension any function of the form

$$u(x,t) = f(x \pm ct) \tag{12}$$

is a solution of the wave equation (1), where $\pm$ defines the direction of the propagating wave. Hence, a polynomial in terms of $(x \pm ct)$ seems to be a natural choice for the approximation u^h. On a reference space–time element of size h and Δt in spatial and temporal direction, respectively, we choose polynomials in $(x - ct)$ and $(x + ct)$ for the shape functions. The approximation u^h may then be written as

$$\begin{aligned} u^h(x,t) &= u_0 + \frac{1}{h}(x-ct)\,u_1 + \frac{1}{h^2}(x-ct)^2\,u_2 + ... + \frac{1}{h^p}(x-ct)^p\,u_p \\ &+ \frac{1}{h}(x+ct)u_{p+1} + \frac{1}{h^2}(x+ct)^2 u_{p+2} + ... + \frac{1}{h^p}(x+ct)^p\,u_{2p} \\ &= \sum_{i=0}^{2p} N_i(x,t)\,u_i\ , \end{aligned} \tag{13}$$

where

$$\begin{aligned} N_0 &= 1, \\ N_l &= \frac{1}{h^l}\,(x-ct)^l\ , \quad l = 1, ..., p\ , \\ N_m &= \frac{1}{h^{m-p}}\,(x-ct)^{m-p}\ , \quad m = p+1, ..., 2p. \end{aligned}$$

The terms $(x \pm ct)^i$ are scaled with $1/h^i$ in order to obtain non-dimensional basis functions and to improve conditioning of the resulting system. The nine element basis functions up to order $p = 4$ are depicted on a reference element in Figure 3.

It should be emphasized here that the governing variational form allows for a variety of other basis functions. Particularly, if the system excitation includes a distinct content at or around a specific wave number k, basis functions of type $\sin(kx \pm ct)$ and $\cos(kx \pm ct)$ appear to be attractive. However, without the knowledge of a particular frequency content in the system excitation and response, the basis functions in equation (13) seem most appropriate.

3.2. Approximation of the Lagrange multipliers

Considering two neighboring elements within a space–time slab, the Lagrange multiplier λ in the variational form can be identified as the normal derivative of u. This motivates to chose λ^h as a good approximation of $\partial u^h/\partial x$ (cf. [31]).

With the previously chosen basis functions for u^h of order p (cf. (13)), the derivative $\partial u^h/\partial x$ is a polynomial of order $p-1$ in t at the element edges $\Gamma_{e,e'}$. This suggests that the appropriate Lagrange multiplier approximation is at most of order $(p-1)$. However, further considerations regarding the stability and efficiency generally limit the choice of λ^h and the corresponding number of Lagrange multiplier degrees of freedom. The key stability issues for hybrid formulations such as (11) are described by the *inf-sup* condition [36, 37]. The outcome of this condition can be expected to relate the number of Lagrange multiplier degrees of freedom and the number of wave basis approximations. An extensive survey of techniques for approximating Lagrange multipliers, including theoretical results pertaining to the *inf-sup* condition, can be found in [38]. The fact that the discrete problem becomes overconstrained if the number of Lagrange multipliers exceeds the number of wave basis functions may be seen as a global condition. Given that an edge $\Gamma_{e,e'}$ is shared by two elements except at the boundaries of the computational domain, this global condition implies $n_\lambda \leq 2n_E$, where n_λ

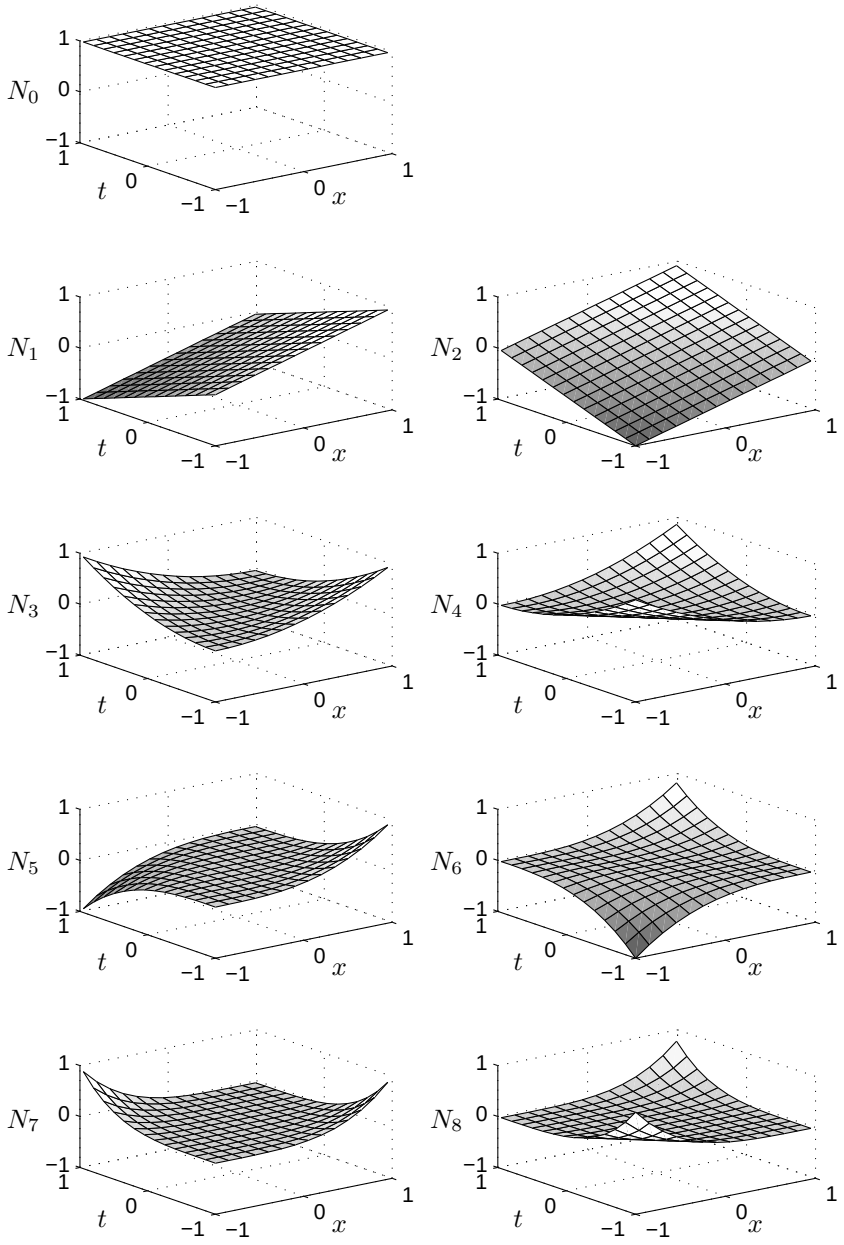

Figure 3. Basis functions up to order $p = 4$ for $c = 1$ on a reference element $\Omega_e \times I = [-1, 1] \times [-1, 1]$.

and n_E are the restrictions of the corresponding function spaces to one element. However, in order to increase efficiency one may tend to further reduce the number of Lagrange multipliers.

Thus, the Lagrange multipliers along an element edge $\Gamma_{e,e'}$ to be used in conjunction with the element basis functions in equation (13) can be written in terms of standard finite element shape functions $\Phi_i(t)$, i.e.

$$\lambda^h(t) = \sum_{i=0}^{p_\lambda} \Phi_i(t)\, \lambda_i \ , \tag{14}$$

where p_λ is the order of the Lagrange multiplier approximation.

3.3. Algebraic formulation

Using the approximations described above and choosing identical trial and test functions leads to discrete versions of equations (11) and (10), that can be written in matrix form as

$$\begin{bmatrix} \mathbf{K}_a & \mathbf{K}_b \\ \mathbf{K}_b^T & \mathbf{0} \end{bmatrix} \begin{bmatrix} \mathbf{u} \\ \lambda \end{bmatrix} = \begin{bmatrix} \mathbf{f} \\ \mathbf{0} \end{bmatrix}. \tag{15}$$

The contribution from an element e with degrees of freedom $[\mathbf{u}^e\ \lambda^e]^T$ to the resulting system matrix and right hand side vector are given by

$$\begin{bmatrix} \mathbf{k}_a^e & \mathbf{k}_b^e \\ \mathbf{k}_b^{e^T} & \mathbf{0} \end{bmatrix}, \begin{bmatrix} \mathbf{f}^e \\ \mathbf{0} \end{bmatrix}, \tag{16}$$

where the corresponding entries of the matrices $\mathbf{k}_a^e$ and $\mathbf{k}_b^e$ and the vector $\mathbf{f}^e$ are given by

$$\begin{aligned} k_{a,ij}^e &= \int_{t_n}^{t_{n+1}} \int_{\Omega_e} (u_{x,j}\ \dot{w}_{x,i} + \frac{1}{c^2} \ddot{u}_j\ \dot{w}_i)\ dx\, dt \\ &\quad + \int_{\Omega_e} \frac{1}{c^2} \dot{u}_j(t_n^+)\ \dot{w}_i(t_n^+)\ dx + \int_{\Omega_e} u_{x,j}(t_n^+)\ w_{x,i}(t_n^+)\ dx, \end{aligned} \tag{17}$$

$$k_{b,ij}^e = \sum_{e<e'} \int_{t_n}^{t_{n+1}} [\![\dot{w}_i(\Gamma_{e,e'})]\!]\ \lambda_j\ dt, \tag{18}$$

$$f_i^e = \int_{\Omega_e} \frac{1}{c^2} \dot{u}(t_n^-)\ \dot{w}_i(t_n^+)\ dx + \int_{\Omega_e} u_x(t_n^-)\ w_{x,i}(t_n^+)\ dx. \tag{19}$$

3.4. Regularization and reduced approximation

Since both trial and test functions only appear in form of spatial and/or temporal derivatives in the variational form (11), all constant terms in the approximations vanish in the weak form, rendering a singular matrix $\mathbf{k}_a$ and subsequently a singular system of equations (15). There are several ways to regularize either the element matrices $\mathbf{k}_a$ or the global system in equation (15). Here, the following approach is proposed. In order to obtain a non-singular matrix $\mathbf{k}_a$, the constant terms of the approximation u_h are dropped when assembling the element matrices, leading to the reduced approximation

$$\tilde{u}^h(x,t) = \sum_{i=1}^{2p} N_i(x,t)\, u_i \ , \tag{20}$$

where the shape functions N_i, $i = 1, .., 2p$, remain unaltered.

The constant term u_0 of the full approximation on each element may be computed from an additional constraint that enforces continuity of the numerical solution for one point $\tau = (x, t)$ on an edge $\Gamma_{e,e'}$, i.e.

$$\sum_{i=0}^{2p} N_i(\tau) u_i^e \quad = \quad \sum_{i=0}^{2p} N_i(\tau) u_i^{e'} \quad \tau \in \Gamma_{e,e'}. \tag{21}$$

Once $\tilde{u}^h$ is known, the constant terms u_0 can be evaluated starting from the Dirichlet boundary condition on one side of a space–time slab on element level by rearranging (21). For two neighboring elements e and e', this condition yields

$$u_0^{e'} = \sum_{i=0}^{2p} N_i(\tau) u_i^e - \sum_{i=1}^{2p} N_i(\tau) u_i^{e'}, \quad \tau \in \Gamma_{e,e'}. \tag{22}$$

For the computations presented here, we have chosen τ to be located at the end of a time step, i.e. $t = t_{n+1}^-$.

As an example, Figure 4 shows the numerical solutions at the end of a time step obtained using the approximation in (20) and after computing and adding the constant terms u_0.

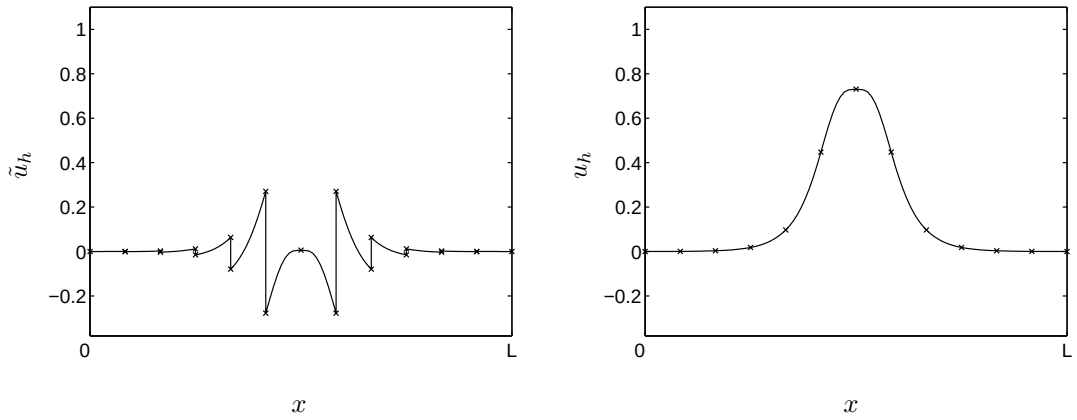

Figure 4. Numerical solution at the end of a time step excluding (a) and including (b) the constant terms in the element basis functions

Note that the consideration of the constraint (21) by means of additional Lagrange multipliers within the weak formulation corresponds to another way to regularize the resulting system of equations in a general case of non-homogeneous Dirichlet boundary conditions.

4. IMPLEMENTATION

4.1. Static condensation

Since the element approximation is based on discontinuous functional spaces, the element degrees of freedom associated with u_h can be statically condensed. This simplifies the formulation, reduces its computational costs, and improves its conditioning.

Since the field u_h^e for an element e can be written as

$$\mathbf{u}^e = (\mathbf{k}_a^e)^{-1} \left(\mathbf{f}^e - \mathbf{k}_b^e \, \lambda^e\right), \tag{23}$$

only the following matrices

$$\tilde{\mathbf{k}}^e = -\mathbf{k}_b^{e^T} \, (\mathbf{k}_a^e)^{-1} \, \mathbf{k}_b^e \tag{24}$$

and vectors

$$\tilde{\mathbf{f}}^e = -\mathbf{k}_b^{e^T} \, (\mathbf{k}_a^e)^{-1} \, \mathbf{f}^e \tag{25}$$

are build and assembled into the global system

$$\tilde{\mathbf{K}} \, \lambda = \tilde{\mathbf{f}}. \tag{26}$$

Hence, equation (26) is first solved for the Lagrange multipliers. The solution for the eliminated field is then obtained from equation (23) and the condition (21) as a postprocessing step within each element.

4.2. Evaluation of the integral quantities

The conventional space–time finite element methods require the evaluation of integral terms that are defined over space and time. The integration is generally carried out numerically by means of quadrature rules. At low approximation orders the matrix assembly usually represents only a marginal part of the computational costs, which are mostly governed by the solution of the resulting system of equations. With increasing orders of the element shape functions, the numerical integration becomes increasingly expensive and may represent a considerable portion of the overall costs. With our specific choice of the element shape functions, the integrals over the space–time elements can be reduced to boundary integrals that may be evaluated analytically (see e.g. [32]). This simplification leads to a significant reduction of the computational costs in the matrix assembly process.

Consider the computation of the element matrices $\mathbf{k}_a^e$ as given in equation (17). This includes the term

$$\int_{t_n}^{t_{n+1}} \int_{\Omega_e} (u_x^h \, \dot{w}_x^h + \frac{1}{c^2} \ddot{u^h} \, \dot{w}^h) \, dx \, dt. \tag{27}$$

Using integration by parts yields

$$\int_{t_n}^{t_{n+1}} \int_{\Omega_e} (u_x^h \, \dot{w}_x^h + \frac{1}{c^2} \ddot{u^h} \, \dot{w}^h) \, dx \, dt = \int_{t_n}^{t_{n+1}} \int_{\Omega_e} (-u_{xx}^h + \frac{1}{c^2} \ddot{u^h}) \, \dot{w}^h \, dx \, dt + \int_{t_n}^{t_{n+1}} \left[u_x^h \, \dot{w}^h\right]_{\Gamma_{e_1}}^{\Gamma_{e_2}} \, dt, \tag{28}$$

where Γ_{e_1} and Γ_{e_2} refer to the spatial boundaries of element e. A crucial point of our method is to intentionally chose basis functions that are solutions of the homogeneous wave equation. Hence, the first integral term on the right hand side of equation (28) vanishes, i.e.

$$\int_{t_n}^{t_{n+1}} \int_{\Omega_e} (u_x^h \, \dot{w}_x^h + \frac{1}{c^2} \ddot{u^h} \, \dot{w}^h) \, dx \, dt = \int_{t_n}^{t_{n+1}} \left[u_x^h \, \dot{w}^h \right]_{\Gamma_{e_1}}^{\Gamma_{e_2}} \, dt, \tag{29}$$

which transforms the integral over the space–time element into a boundary integral.

5. NUMERICAL RESULTS

To assess the performance of the newly developed method, we consider here two instances of the initial/boundary value problem given in (1)–(3). The first one is a standing wave problem in a one dimensional acoustic domain of length L, where the dispersion and dissipation characteristics of the numerical solution may be inferred from the results. The second test problem corresponds to propagating waves of the form $\mathrm{sech}(x \pm ct)$, i.e. representing a rather broad band excitation, which may give rise to spurious oscillations in the numerical solution [39, 40]. For all computations, the speed of sound c is of unit value.

In order to highlight the superior performance of the space–time DGM formulation presented here, numerical results are compared with those obtained using conventional space–time elements based on time discontinuous formulations (cf. [13, 17, 18]). The conventional elements are denoted here by Q_2 and Q_3 for second and third order approximations in space and time, respectively. However, some considerations should be made when comparing the complexity of the different elements for assembling and solving the global system. Employing the static condensation as described in section 4.1, the size of the resulting system is significantly reduced. It is noted here, that a static condensation may to some extent also be employed when using the conventional space–time elements Q_2 and Q_3. Since coupling of the degrees of freedom only occurs along element edges $\Gamma_{e,e'}$ the remaining degrees of freedom may be statically condensed. The space–time discontinuous elements are associated with high approximation orders p which lead to a rather large number of element degrees of freedom and consequently increases costs for the static condensation. Furthermore high approximation orders generally increase the costs for the evaluation of integral expressions during the system assembly. However, using the transformation described in section 4.2, the costs for the integration are considerably reduced. Assuming that the solution of the resulting system dominates the overall computational costs, the space–time element denoted Q_2 may be compared with discontinuous space–time elements that include second order approximations of the Lagrange multipliers, i.e. $p_\lambda = 2$, since both element types lead to the same number of degrees of freedom when used with identical mesh resolutions. Similarly, the cubic element Q_3 may be compared with discontinuous space–time elements with approximations of the Lagrange multiplier up to cubic order, i.e. $p_\lambda = 3$.

In the remainder of this paper, we will refer to the quadratic and cubic space–time elements based on the time discontinuous Galerkin method as Q_2 and Q_3 elements, respectively, and we will refer to the newly developed elements as *stDGM*-p_w-p_λ elements (or space–time DGM elements) with orders p_w for the approximation of the solution and p_λ the Lagrange multiplier approximation. The number of element basis functions and the total number of degrees of freedom (dof) in the condensed system for the different element types that were used in the one dimensional example problems of this section are given in Table I.

Table I. Number of element basis functions and total number of dof in a space–time slab with n elements in one space dimension

Element	Number of element basis functions	Number of dof in the condensed system
$stDGM-3-1$	7	$2\,(n+1)$
$stDGM-5-2$	11	$3\,(n+1)$
$stDGM-7-3$	15	$4\,(n+1)$
Q_2	9	$3\,(n+1)$
Q_3	16	$4\,(n+1)$

The comparison of the results in all example problems is based on a relative nodal L^1-error defined by $|u^{ex}-u^h|_1/|u^{ex}|_1$.

5.1. Standing wave problem

The standing wave problem considered in this section has the initial conditions

$$\begin{aligned} U_0 &= \sin\left(n\pi\, x/L\right),\ n\in\mathbb{N}, \\ \dot{U}_0 &= 0, \end{aligned} \tag{30}$$

where n is the number of half sin waves in the domain. The exact solution u^{ex} is then given by

$$u^{ex} = \frac{1}{2}\left(\sin\left(n\pi\left(x-ct\right)/L\right)+\sin\left(n\pi\left(x+ct\right)/L\right)\right). \tag{31}$$

Analytical solutions of the governing PDE for $n=2$ are depicted in Figure 5 at four consecutive time steps.

Figure 6 depicts the relative error and the number of degrees of freedom for various element types, where the number of degrees of freedoms corresponds to the size of the resulting statically condensed system. The results in Figure 6 were obtained for the standing wave problem with $L=2$ and $n=20$, i.e. 10 wave lengths in the computational domain (cf. (31)). The relative error was computed at a simulation time $t=50$, which represents 250 periods of the system and element lengths in temporal direction, i.e. time step sizes, of $\Delta t=h/(2c)$ and $\Delta t=h/c$ were chosen. Note that the system responds at a single frequency, where the non-dimensional wavenumber corresponds to $kL\approx 60$.

The results depicted in Figure 6 show the outstanding performance of the space–time DGM elements. Comparing the number of degrees of freedom needed to reach the relative error level of 10^{-2}, the space–time DGM with $p_w=7$ and $p_\lambda=3$ requires roughly four times fewer degrees of freedom than the comparable cubic element Q_3. In the depicted range for the number of degrees of freedom, the second order element Q_2 does not provide reasonably accurate results.

A comparison of the $stDGM-7-3$ element and the cubic element Q_3 for different vibrational modes with $n=20$, $n=30$, and $n=40$ is given in Figure 7. The vibrational modes correspond to non-dimensional wave numbers of $kL\approx 60$, $kL\approx 90$, and $kL\approx 120$. From the slope of the graphs in Figure 7 it can be seen that the $stDGM-7-3$ element exhibits higher convergence rates than the cubic space–time element Q_3. Comparing the number of degrees of freedom at

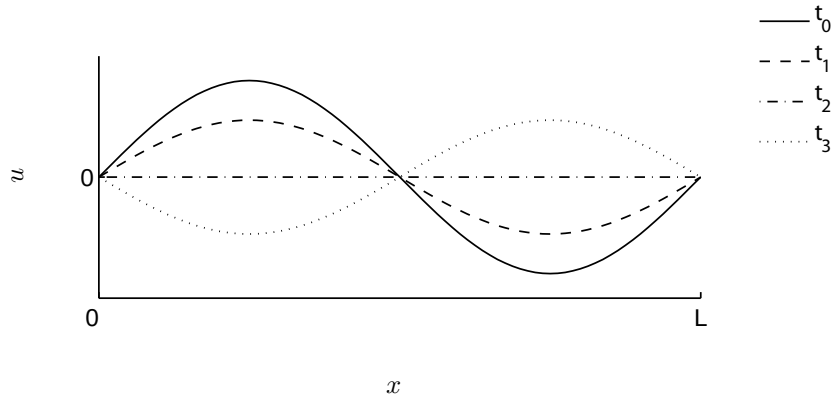

Figure 5. The solution u at four consecutive time steps with $t_0 < t_1 < t_2 < t_3$ of the standing wave problem with $n = 2$. The solid line corresponds to $t_0 = 0$.

a relative error level of 10^{-2}, the $stDGM - 7 - 3$ element requires roughly 3.5 times fewer degrees of freedom for $\Delta t = h/(2c)$ and 3 times fewer degrees of freedom for $\Delta t = h/c$ than the Q_3 element. The advantage of the $stDGM - 7 - 3$ element appears to slightly increase for higher vibrational modes, i.e. with increasing non-dimensional wave number.

For a discretization with $n_{el} = 40$ elements and $\Delta t = h/(2c)$ the system response was monitored at $x = L/40$. In the vicinity of $t = 100$ (which corresponds to 4000 time steps for 500 periods) results for the cubic element Q_3 and the space–time DGM element with $p_w = 5$ and $p_\lambda = 2$ are depicted in Figure 8 together with the exact solution as given by equation (31).

Clearly the result for the Q_3 elements imply numerical dispersion as well as dissipation, whereas the space–time DGM exhibits excellent quality of the numerical results. The numerical results obtained with the space–time DGM and the exact solution are almost perfectly aligned. It is pointed out here that the space–time DGM element with $p_\lambda = 2$ that has been employed leads to a resulting system with fewer degrees of freedom than the Q_3 element, yet it improves the accuracy of results significantly.

5.2. Propagating wave problem

The example problem investigated here is a propagating wave with initial conditions

$$\begin{aligned} U_0 &= \operatorname{sech}\left(20\left(x - L/2\right)\right), \\ \dot{U}_0 &= 0. \end{aligned} \tag{32}$$

These lead to the exact solution

$$u^{ex} = \frac{1}{2}\left(\operatorname{sech}\Big(20\big(\,(x - L/2) - ct\big)\Big) + \operatorname{sech}\Big(20\big(\,(x - L/2) + ct\big)\Big)\right). \tag{33}$$

While the first example problem includes a system response with a single frequency, the initial conditions in (32) represent a broad band excitation of the system. Note that the Fourier

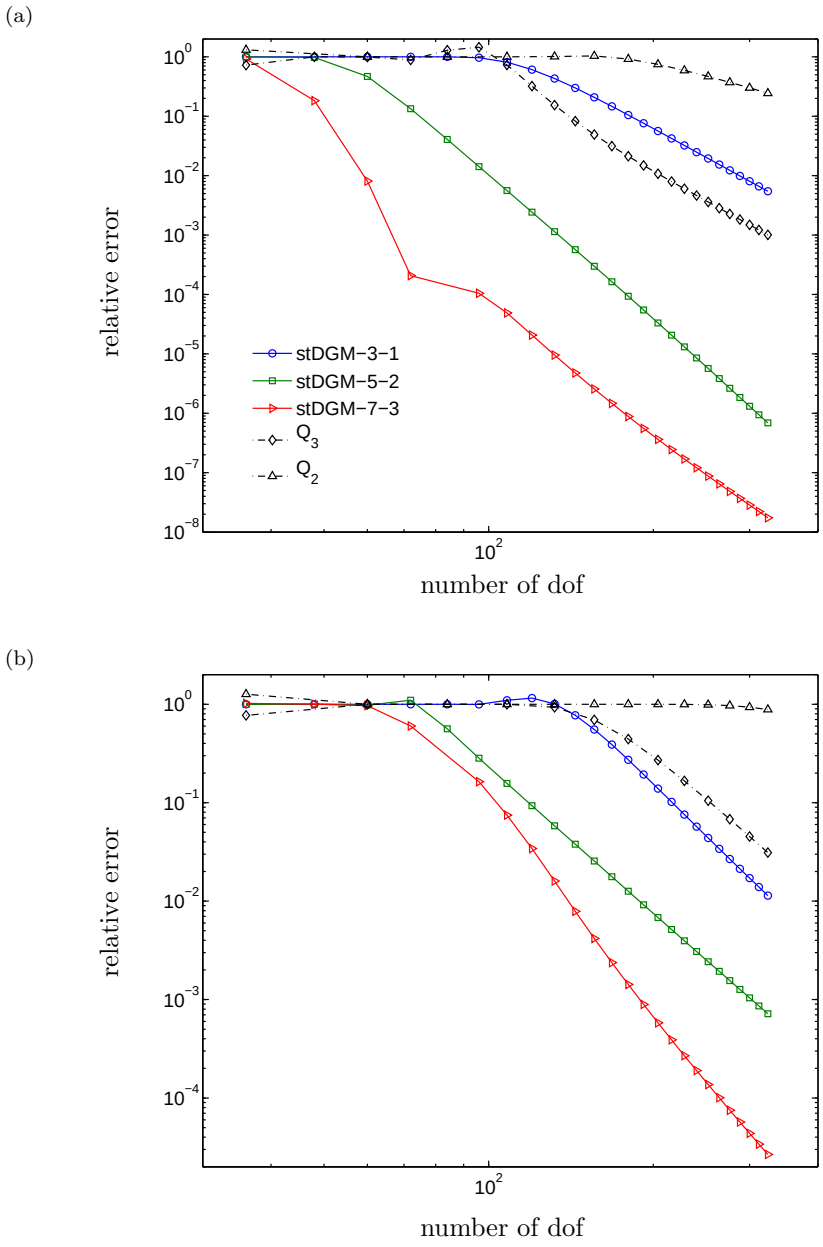

Figure 6. Relative error in nodal L^1-norm at time $t = 50$ and number of degrees of freedom for different elements based on spatially continuous and discontinuous approximations for two different time step sizes: (a) $\Delta t = h/(2c)$ and (b) $\Delta t = h/c$

(a)

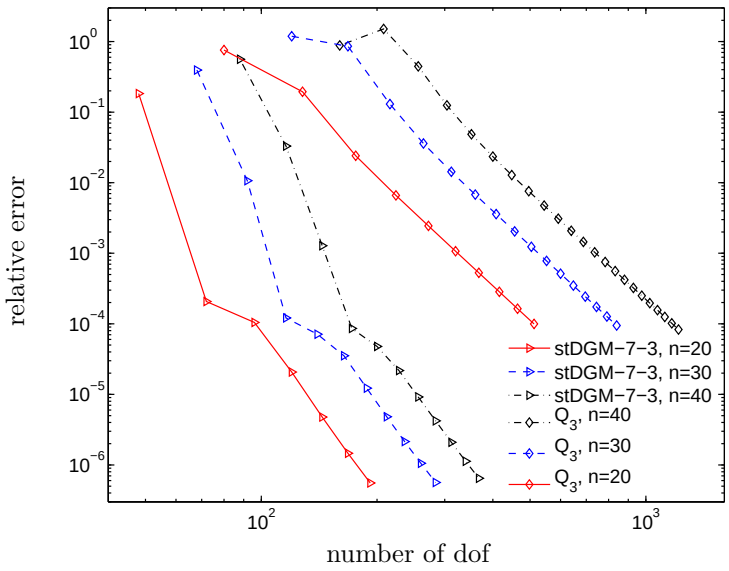

(b)

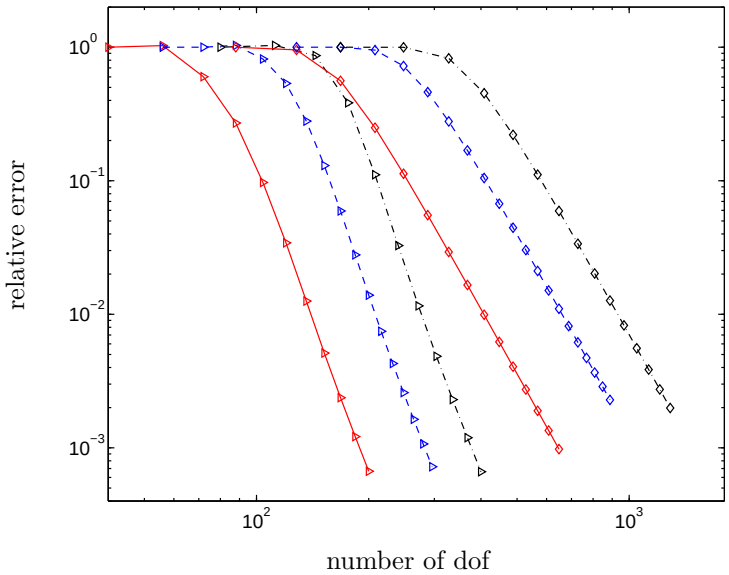

Figure 7. Relative error in nodal L^1-norm at time $t = 50$ and number of degrees of freedom for elements based on spatially continuous and discontinuous approximations and different vibration modes for two time step sizes: (a) $\Delta t = h/(2c)$ and (b) $\Delta t = h/c$

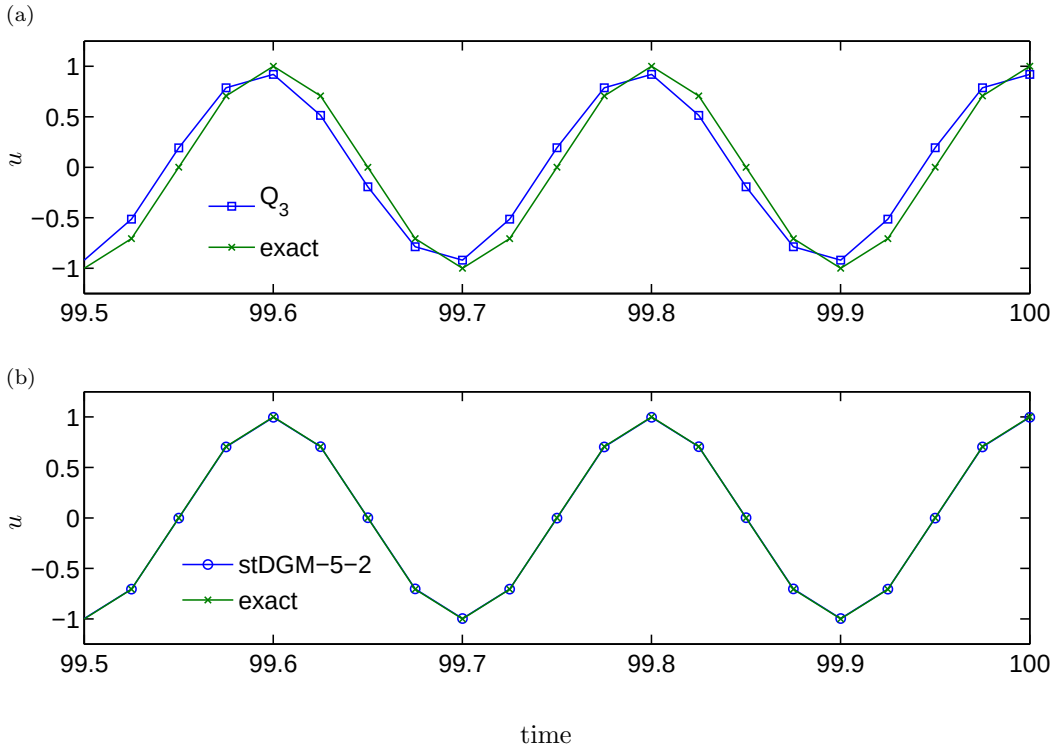

Figure 8. Exact solution and numerical results at $x = L/40$ for the standing wave problem. The Numerical results are obtained using space–time elements Q_3 (a) and the space–time DGM elements with $p_W = 5$ and $p_\lambda = 2$ (b).

transform of a function $\mathrm{sech}(at)$ is given by $1/a\sqrt{\pi/2}\,\mathrm{sech}(\pi\omega/(2a))$, where ω is the circular frequency. Hence, the Fourier transform of the initial wave form represents a sech function centered at the origin. Assuming that the signal contains significant content in the frequency range from 0 to 5 Hz, the minimum wave length is given by 1/5. The analytical solution for the propagating wave problem at four consecutive time steps are depicted in Figure 9.

Convergence results for the propagating wave problem with $L = 12$ are given in Figure 10, where the relative error was evaluated at $t = 4$ for time steps sizes of $\Delta t = h/(2c)$ and $\Delta t = h/c$.

For this example problem, all three types of space–time DGM elements perform better than the conventional space–time elements Q_2 and Q_3. Comparing the $stDGM$-7-3 element and the Q_3 element at an error level of 10^{-2}, the latter one requires roughly three times more degrees of freedom for a time step size of $\Delta t = h/(2c)$ and twice more degrees of freedom for $\Delta t = h/c$. Similarly, the comparison of the $stDGM$-5-2 element and the Q_2 element indicates a 3.5-fold reduction of the degrees of freedom for the two time step sizes of $h/(2c)$ and h/c, when using

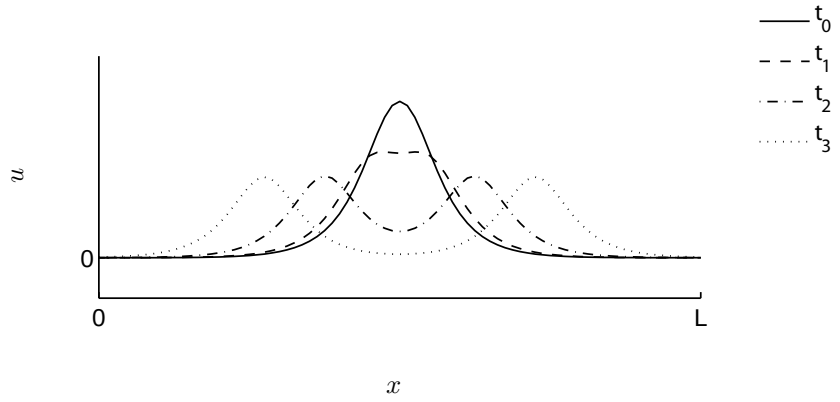

Figure 9. The solution u at four consecutive time steps with $t_0 < t_1 < t_2 < t_3$ for the propagating wave problem. The solid line corresponds to the initial time step at $t = 0$.

the space–time DGM element .

The field $u(x, 4)$ is depicted in Figure 11 together with the exact solution for a rather coarse discretization with $n_{el} = 108$ elements. The exact solution over the whole domain at $t = 4$ is depicted in the upper left part of Figure 11. Comparisons with the numerical solutions are shown in the lower part of the figure.

The solution obtained with the space–time DGM elements is almost perfectly aligned with the exact solution, whereas the Q_3 element fails to provide reasonably accurate results. Furthermore, the spurious oscillations that generally occur in the numerical solution are about two orders of magnitude less for the space–time discontinuous element with $p_w = 7$ and $p_\lambda = 3$.

To further highlight the potential of the space–time DGM method developed here, the exact solution and the numerical solution for the wave propagation problem with $L = 200$, $h = L/2000$ and $\Delta t = h/(2c)$ are shown at time $T = 95$ in Figure 12. The length of the computational domain corresponds to 1000 times the assumed minimum wave length of 1/5. While the cubic space–time element Q_3 yields inadequate results at the given mesh resolution, the numerical solution for the $stDGM - 7 - 3$ element is in very good agreement with the analytical solution, where the nodal L^1-error is less than 3%.

6. CONCLUSION

A new space–time discontinuous Galerkin method for the solution of the acoustic wave equation in the time domain has been presented. The method may be interpreted as a space–time variant of the discontinuous enrichment method [9], where a key feature is the use of solutions of the wave equation as element shape functions. The specific choice of element basis functions is enabled by means of a variational formulation that allows for discontinuities in the temporal as well as the spatial direction. Continuity of the numerical solution in space is weakly enforced by means of Lagrange multipliers. The discontinuous definition of the element shape

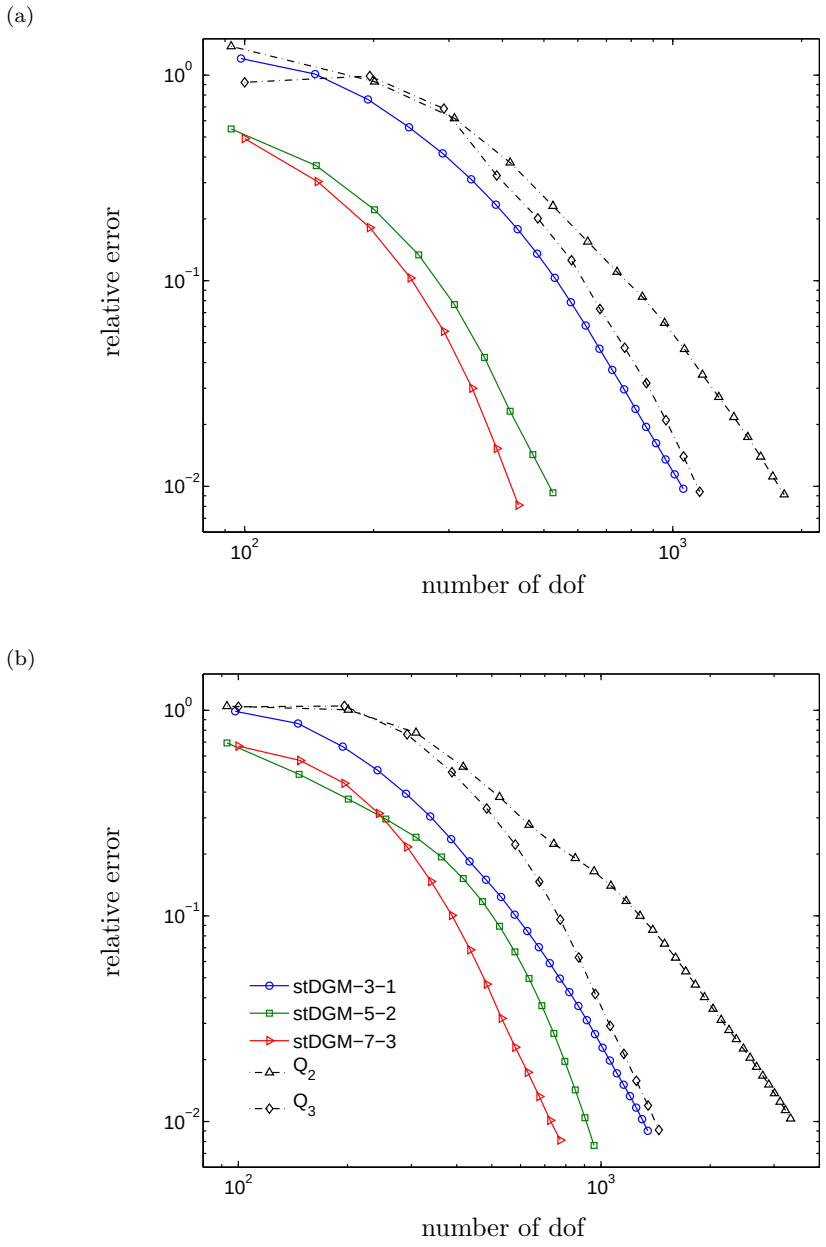

Figure 10. Relative error in nodal L^1-norm at time $t = 4$ and number of degrees of freedom for the propagating wave problem solved with two different time step sizes: (a) $\Delta t = h/(2c)$ and (b) $\Delta t = h/c$

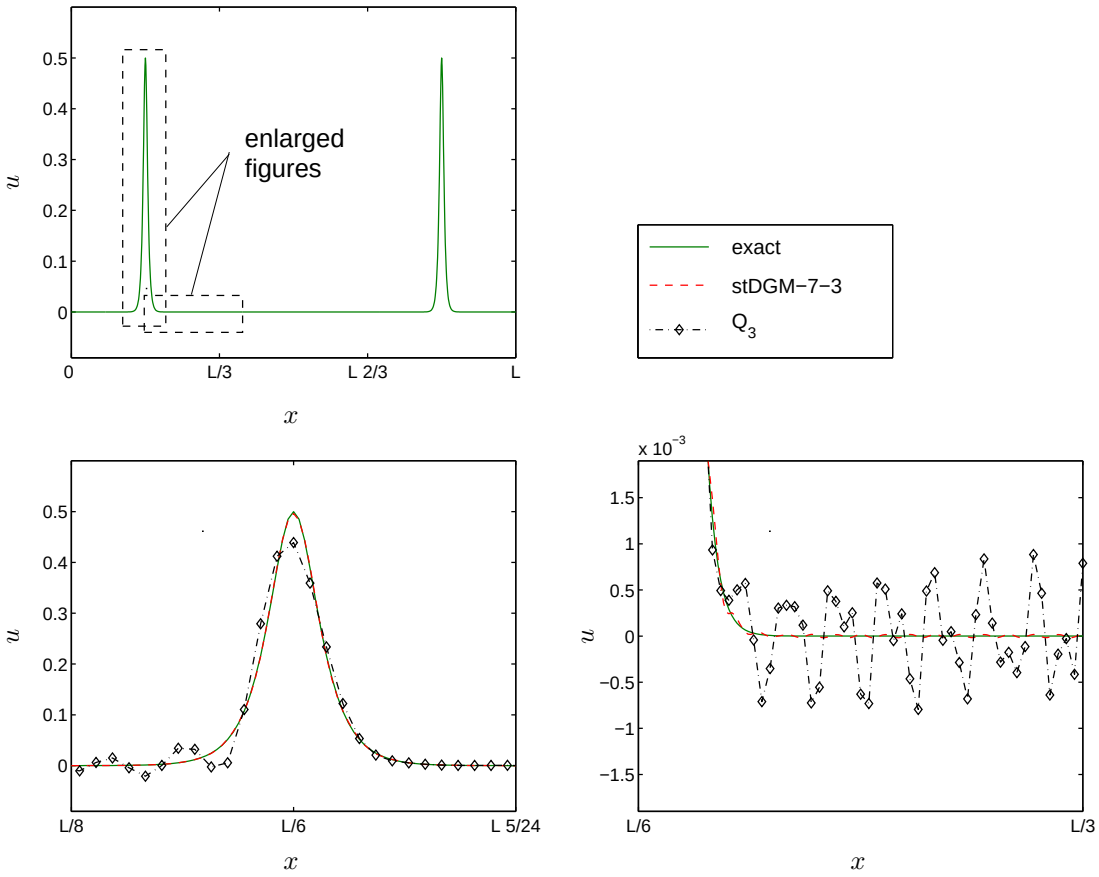

Figure 11. Exact solution and numerical solution at $t = 4$ for the propagating wave problem with $L = 12$.

approximations allows for a static condensation, which significantly reduces the computational costs. Furthermore, the choice of free space solutions of the governing differential equation enables an efficient and analytically exact evaluation of integral terms, when computing the contributions from an element to the global system.

The numerical examples in one space dimension show a great potential for the efficient solution of wave propagation phenomena in the time domain. In comparisons with conventional space–time elements based on the time discontinuous Galerkin method, the newly developed elements give superior performance. Comparing the number of degrees of freedom at engineering accuracy level, our space–time discontinuous elements require up to 4 times fewer degrees of freedom than the conventional space–time elements of comparable order. It is further emphasized here, that comparisons of the different element types have been carried out for a fixed ratio of $\Delta t/h$. Hence, a larger spatial element size h also results in larger time step

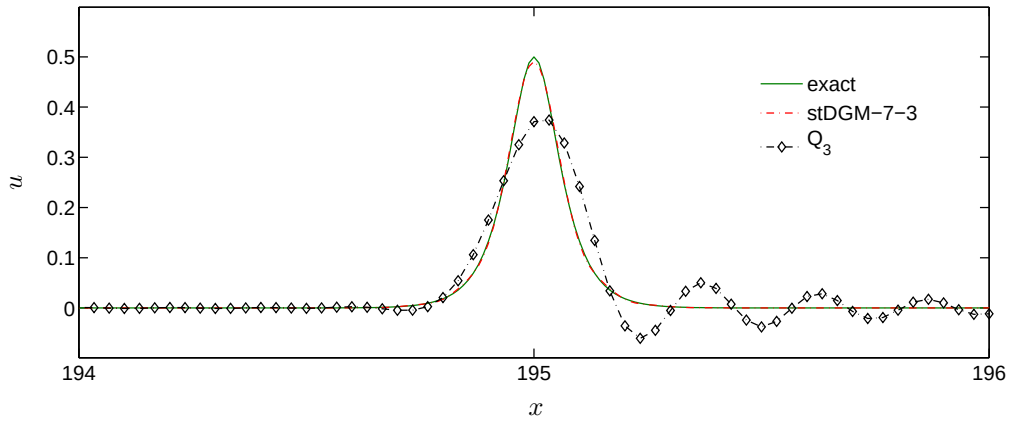

Figure 12. Exact solution and numerical solution at $t = 95$ for the propagating wave problem with $L = 200$.

sizes Δt. As a consequence, the space–time discontinuous elements developed here do not only reduce the cost for solving the resulting system in each space–time slab, but also reduces the number of time steps (i.e. the necessary total number of linear solves) when simulating over a certain time period.

Future work will primarily focus on the extension of the approach for problems in two and three space dimensions, further investigations regarding the approximations with other wave basis functions, and the adaption of the method for explicit time integration schemes.

ACKNOWLEDGEMENTS

The work has been supported by a fellowship within the post-doc program of the German Academic Exchange Service (DAAD) under contract D/06/44695 as well as a research grant by the Office of Naval Research (ONR) under contract N00014-05-1-0204-1. The support is greatfully acknowledged.

REFERENCES

1. G. C. Cohen. *Higher-Order Numerical Methods for Transient Wave Equations*. Springer, Berlin, 2002.
2. M. Käser and M. Dumbser. An arbitrary high-order discontinuous galerkin method for elastic waves on unstructures meshes - i. the two-dimensional isotropic case with external source terms. *Geophysical Journal International*, 166:855–877, 2006.
3. D. A. Arnold, F. Brezzi, B. Cockburn, and L. D. Marini. Unified analysis of discontinuous Galerkin methods for elliptic problems. *SIAM Journal on Numerical Analysis*, 39:1749–1779, 2002.
4. S. J. Sherwin, R. M. Kirby, J. Peiró, R. L. Taylor, and O. C. Zienkiewicz. On 2D elliptic discontinuous Galerkin methods. *International Journal for Numerical Methods in Engineering*, 65:752–784, 2006.
5. F. Brezzi, B. Cockburn, L. D. Marini, and E. Süli. Stabilization mechanisms in discontinuous Galerkin finite element methods. *Computer Methods in Applied Mechanics and Engineering*, 195:3293–3310, 2006.
6. B. Cockburn, G. E. Karniadakis, and C.-W. Shu. The development of discontinuous Galerkin methods. In B. Cockburn, G. E. Karniadakis, and C.-W. Shu, editors, *Diskontinuous Galerkin methods – Theory, computation and application*, pages 3–50. Springer, Berlin, 2000.

7. M. Delfour, W. Hager, and F. Trochu. Discontinuous Galerkin methods for ordinary differential equations. *Mathematics of Computation*, 36:455–473, 1981.
8. Johnson C., U. Nävert, and J. Pitkäranta. Finite element methods for linear hyperbolic problems. *Computer Methods in Applied Mechanics and Engineering*, 45:285–312, 1984.
9. C. Farhat, I. Harari, and L. P. Franca. The discontinuous enrichment method. *Computer Methods in Applied Mechanics and Engineering*, 190:6455–6479, 2001.
10. M. J. Grote, A. Schneebeli, and D. Schötzau. Discontinuous Galerkin finite element method for the wave equation. *SIAM Journal on Numerical Analysis*, 44:2408–2431, 2006.
11. C. E. Baumann and Oden J. T. A discontinuous hp finite element method for the Euler and Navier–Stokes equations. *International Journal for Numerical Methods in Fluids*, 31:79–95, 1999.
12. Réviere B. and M. F. Wheeler. Discontinuous finite element methods for acoustic and elastic wave problems. *Contemporary Mathematics*, 329:271–282, 2003.
13. T. J. R. Hughes and G. M. Hulbert. Space-time finite element methods for elastodynamics: formulation and error estimates. *Computer Methods in Applied Mechanics and Engineering*, 66:339–363, 1988.
14. P. Monk and Richter G. R. A discontinuous Galerkin method for linear symmetric hyperbolic systems in inhomogeneous media. *Journal of Scientific Computing*, 22–23:443–477, 2005.
15. M. Ainsworth, P. Monk, and W. Muniz. Dispersive and dissipative properties of discontinuous Galerkin finite element methods for the second-order wave equation. *Journal of Scientific Computing*, 27:5–40, 2006.
16. E. T. Chung and B. Engquist. Optimal discontinuous Galerkin methods for wave propagation. *SIAM Journal on Numerical Analysis*, 44:2131–2158, 2006.
17. G. M. Hulbert and T. J. R. Hughes. Space-time finite element methods for second-order hyperbolic problems. *Computer Methods in Applied Mechanics and Engineering*, 84:327–348, 1990.
18. G. M. Hulbert. Time finite element methods for structural dynamics. *International Journal for Numerical Methods in Engineering*, 33:307–331, 1992.
19. Johnson C. Discontinuous Galerkin finite element methods for second order hyperbolic problems. *Computer Methods in Applied Mechanics and Engineering*, 107:117–129, 1993.
20. French D. A. A space-time finite element method for the wave equation. *Computer Methods in Applied Mechanics and Engineering*, 107:145–157, 1993.
21. X. D. Li and N.-E. Wiberg. Structural dynamic analysis by a time-discontinuous Galerkin finite element method. *International Journal for Numerical Methods in Engineering*, 39:2131–2152, 1996.
22. L. L. Thompson and P. M. Pinsky. A space-time finite element method for structural acoustics in infinite domains. Part 1: Formulation, stability and convergence. *Computer Methods in Applied Mechanics and Engineering*, 132:195–227, 1996.
23. L. L. Thompson and P. M. Pinsky. A space-time finite element method for the exterior acoustic problem. *Journal of the Acoustical Society of America*, 99:3297–3311, 1996.
24. L. L. Thompson and D. He. Adaptive space-time finite element methods for the wave equation on unbounded domains. *Computer Methods in Applied Mechanics and Engineering*, 194:1947–2000, 2005.
25. T. J. R. Hughes and Stewart J. R. A space-time formulation for multiscale phenomena. *Journal of Computational and Applied Mathematics*, 74:217–229, 1996.
26. R. S. Falk and Richter G. R. Explicit finite element methods for symmetric hyperbolic equations. *SIAM Journal on Numerical Analysis*, 36:935–952, 1999.
27. R. S. Falk and Richter G. R. Explicit finite element methods for linear hyperbolic equations. In B. Cockburn, G. E. Karniadakis, and C.-W. Shu, editors, *Diskontinuous Galerkin methods – Theory, computation and application*, pages 209–219. Springer, Berlin, 2000.
28. J. M. Melenk and I. Babuška. The partition of unity finite element method: Basic theory and applications. *Computer Methods in Applied Mechanics and Engineering*, 139:289–314, 1996.
29. O. Cessenat and B. Despres. Application of an ultra weak variational formulation of elliptic pdes to the two-dimensional helmholtz problem. *SIAM Journal on Numerical Analysis*, 35:255–299, 1998.
30. I. Tsukerman. A class of difference schemes with flexible local approximation. *Journal of Computational Physics*, 211:659–699, 2005.
31. C. Farhat, I. Harari, and U. Hetmaniuk. A discontinuous Galerkin method with Lagrange multipliers for the solution of Helmholtz problems in the mid-frequency regime. *Computer Methods in Applied Mechanics and Engineering*, 192:1389–1419, 2003.
32. C. Farhat, P. Weidemann-Goiran, and R. Tezaur. A discontinuous Galerkin method with plane waves and Lagrange multipliers for the solution of short wave exterior Helmholtz problems on unstructured meshes. *Wave Motion*, 39:307–317, 2004.
33. R. Tezaur and C. Farhat. Three-dimensional discontinuous Galerkin elements with Lagrange multipliers for the solution of mid-frequency Helmholtz problems. *International Journal for Numerical Methods in Engineering*, 66:796–815, 2006.
34. L. Zhang, R. Tezaur, and C. Farhat. The discontinuous enrichment method for elastic wave propagation

in the medium-frequency regime. *International Journal for Numerical Methods in Engineering*, 66:2086–2114, 2006.
35. C. Farhat, I. Harari, and U. Hetmaniuk. The discontinuous enrichment method for multiscale analysis. *Computer Methods in Applied Mechanics and Engineering*, 192:3195–3209, 2003.
36. I. Babuška. The finite-element method with Lagrangian multipliers. *Numerische Mathematik*, 20:179–192, 1973.
37. F. Brezzi. The finite-element method with Lagrangian multipliers. *Revue Francaise d'Automatique Informatique Recherche Operationelle*, 8(R2):129–151, 1974.
38. F. Brezzi. *Mixed and hybrid finite element methods*. Springer, New York, 1991.
39. T. Belytschko and R. Mullen. On dispersive properties of finite element solutions. In J. Miklowitz and J. D. Achenbach, editors, *Modern problems in elastic wave propagation*, pages 67–82. Wiley, New York, 1978.
40. L. Jiang and R. J. Rogers. Effects of spatial discretization on dispersion and spurious oscillations in elastic wave propagation. *International Journal for Numerical Methods in Engineering*, 29:1205–1218, 1990.